USEA peripheral nerve recordings predict hand grasping and wrist rotation via firing rate and variance^2 neural features

Danielle Lopez
Department of Electrical and Computer Engineering
University of Utah
Salt Lake City, USA
u1369150@utah.edu

Kolja Klug
Department of Biomedical Engineering
University of Utah
Salt Lake City, USA
u1440697@utah.edu

Luke Son
School of Medicine
University of Utah
Salt Lake City, USA
luke.son@hsc.utah.edu

The long term goal of this research is improved motor decoding from nerve implanted Utah Slanted Electrode Arrays (USEAs) to innovate neuroelectric prostheses. Around 400,000 people in the US have upper limb amputations, which hinder acts of daily living. Amputees without functional residual muscles cannot use the state of the art myoelectric prosthesis, but USEAs can record sensory and motor signals directly from nerves, albeit they are not yet used clinically and previous research has seldom focused on using them for continuous motor decoding. Therefore, we took USEA recordings from the residual median arm nerve of an amputee and extracted firing rate and variance^2 as neural features for a neural network in a novel strategy to predict continuous motor intent from peripheral nerves. We found that firing rate was the best predictor of hand grasping while variance^2 was the best predictor of wrist rotation. Specifically, we found that the two channels with the highest SNRs (Channel 1: 22.7313 (19.7900, 24.3257), Channel 6: 18.7726 (13.7616, 23.4047)) inform hand kinematics. We discovered firing frequency yielded significantly ($p < 0.001$) more accurate predictions of hand grasping ($R^2 = 0.7123 \pm 0.004$ to $R^2 = 0.6215 \pm 0.0037$) while variance-squared yielded significantly ($p < 0.001$) more accurate predictions of wrist rotation ($R^2 = 0.3000 \pm 0.0173$ to $R^2 = 0.07563 \pm 0.0045$). We observed that ANN predictions were more for accurate hand grasping than wrist rotation and that variance^2 input yields continuous predictions. Our results provide the field of neuroprostheses with two strategies of decoding motor intent from peripheral nerves. Furthermore, they can inform electrophysiologists on how to optimize recording techniques for the purposes decoding motor intent.

I. Introduction

Around 400,000 people in the U.S. have upper limb amputations [1]. While non-invasive myoelectric prostheses can help, they often fail to provide naturalistic tactile feedback, and are limited to amputees with intact and active residual muscle [2]. Peripheral nerve implants can provide naturalistic tactile feedback, as well as record motor signals [3,4]. It is therefore imperative to understand motor intent encoded in nerve recordings to innovate accessible prostheses

Intrafascicular implants like the Utah Slanted Electrode Array (USEA) record motor signals and stimulate sensory fibers in peripheral nerves [5]. However, specifically decoding motor intent from peripheral nerves is complicated by adjacent sensory signals [6].

In research nerve recordings are rarely intrafascicular and rarely used to continuously decode motor intent [6]. USEAs are not FDA approved for clinical use but may in research with IRB approval [7]. However, recent work by George et al. demonstrated improved functional longevity of S7 USEAs so they would be more clinically practical [5]. It is imperative to improve motor decoding from peripheral USEAs in order to optimize their future clinical utility.

Our objective was to extract features from a peripheral nerve USEA recording to decode motor intent via an ANN. Uniquely, this research attempts intrafascicular continuous motor decoding rather than sensory decoding and stimulation via peripheral nerve surface implants.. Through this study we found that the two channels with the greatest SNRs could be used as predictors of hand kinematics,. Firing rate neural features yielded more accurate predictions of hand grasping than variance^2, and variance^2 neural features yielded more accurate ANN predictions of wrist rotation than firing rate. We observed that ANN predictions were more accurate for hand grasping than wrist rotation and that variance^2 input yields continuous predictions.

II. Methods

A. Participants

The participant in this study was a 57 year-old, male, left hand dominant, left transradial amputee. [8].

B. Signal Acquisition

A USEA was implanted into the residual left median arm nerve proximal to the elbow. The USEA consisted of 100 electrodes arranged in a 10 x 10 grid on a 4mm x 4mm base. 6 of the channels were selected for analysis in this report. Continuous neural signals from the USEA were filtered to be between 0.3Hz (1st-order high-pass Butterworth filter) and 7500 Hz (3rd-order low-pass Butterworth filter [9]. Neural data was then digitally sampled at 30 kHz and digitally filtered with a 250 Hz 4th-order high-pass Butterworth filter.

Neural signals were recorded via the USEA while the participant was cued to intend to perform a left-hand grasp for ~0.5 seconds, followed by approximately ~0.5 s rest, which was repeated 5 times and immediately followed by a repetition of

the above task except with intent to perform a left-hand wrist rotation.

A neural spike threshold was set to negative four times the standard deviation of the first 20,000 recorded data points (prior to any movement cues) in eah channel. Each instance of neural data crossing below the spike threshold and returning to spike threshold iwas considered a spike.

The signal-to-noise ratio (SNR) in decibels (dB) for each spike event was derived via the following equation [11].

$$\text{SNR (dB)} = 20\log\left(\frac{\text{rms}(\text{Voltage}_{\text{signal}})}{\text{rms}(\text{Voltage}_{\text{noise}})}\right) \quad (1)$$

$\text{Voltage}_{\text{signal}}$ for each spike was comprised of the voltage at the time of each spike and 21 surrounding voltage data points. $\text{Voltage}_{\text{noise}}$ for each channel was comprised of all recorded voltages in that channel. SNRs for each spike were calculated by taking 20 by the log of the rms of $\text{Voltage}_{\text{signal}}$ of that individual spike event by the $\text{Voltage}_{\text{noise}}$ of the corresponding channel. SNRs for each spike were then organized by channel.

C. *Feature Generation*

The first neural feature generated was the firing rate of channels 1 and 6, which was calculated by counting the number of spikes in each channel over a centered 24,000 element moving window. Each sum was then multiplied by 1.25 to obtain the frequency in Hz.

The second neural feature generated was the variance[2] of channels 1 and 6. This feature was calculated by taking the variance of the data points in each channel over a centered 1,000 element moving window. This feature was then smoothed by taking the average of the values over a centered 20,000 element moving window. To normalize the smoothed variance values in each channel were then each divided by mean of the first ten smoothed feature data points (prior to any movement cues). To then set "rest" to zero, for each channel, the minimum value of the processed features in each channel was subtracted from all the processed features in each channel. Lastly, the resulting features were then squared to increase gain and provide the final feature values.

D. *Algorithm and Evaluation*

Neural feature and intended kinematics data were used to train an 11-layer ANN at a learning rate of 0.01 for 1 epoch, to output predictions of intended kinematics.

After test data was passed through the trained neural network, the R^2 values (coefficients of determination) among ANN predictions and intended kinematics were taken for both movements. This was repeated for the second neural feature.. The entire process was repeated for ten trials. The data was used to evaluate ANN prediction accuracy for both features and both movements.

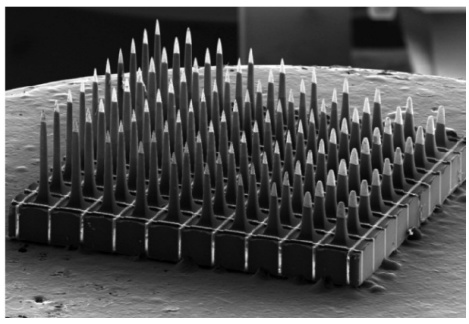

Figure 1. A Utah Slanted Electrode Array (USEA) was implanted in the residual median arm nerve of an amputee. Above is an image of a USEA taken by scanning electron microscope [10].

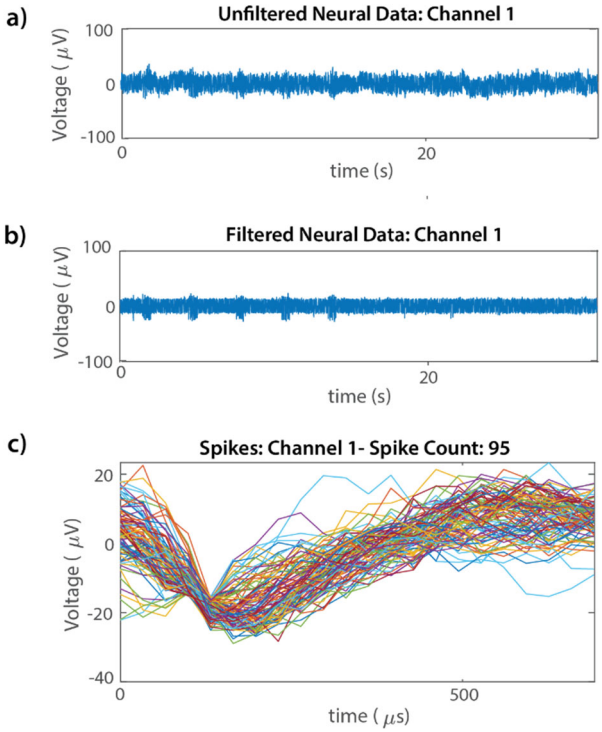

Figure 2. Unfiltered neural data, filtered neural data, and spike waveforms from one USEA channel. a) Example unfiltered voltages recorded from channel 1 of an implanted USEA in the residual median arm nerve of an amputee b) The voltages from part a after filtering the data c) The plotted waveforms of spikes detected from the filtered neural data in part b.

E. *Statistical Analyses*

For both SNR and R^2 analyses, histograms and Anderson-Darling tests were performed to assess (N=10 for all R^2 groups, for SNR groups: N = 95 (channel 1), N = 85 (channel 2), N = 67 (channel 3), N = 33 (channel 4), N = 48 (channel 5), N = 151 (channel 6)) normality. None of the SNR data groups had normal distributions, and there were 6 groups, so a nonparametric ANOVA was performed on the data. Corrections for multiple comparisons were performed using the multcompare function in MATLAB. All R^2 data groups were parametric, so an unpaired t-test was performed to compare performance of the two neural features for both movements.

III. RESULTS

A. *Channels 1 and 6 had greatest signal-to-noise ratios and were used for motor decoding*

We implanted USEA in the residual median left arm nerve of an amputee. We then assessed the SNRs of six USEA channels. We used equation (1) to calculate the SNR for each spike event [11], with $Voltage_{sgnal}$ being the values recorded at and around the spike event, and $Voltage_{noise}$ being all the voltages recorded in that channel. We then grouped the SNRs by channel for data analysis (Fig 3). The medians and interquartile ranges (IQRs) of each channel are as follows – 1: 22.7313 (19.7900, 24.3257), 2: 18.5668 (9.0805, 21.7921), 3: 7.8637 (6.3570, 10.5471), 4: 16.3945 (12.8879, 17.3291), 5: 7.7265 (6.0127, 11.0485), 6: 18.7726 (13.7616, 23.4047). Figure 3 displays significance among channels.

B. *Firing rate is a greater predictor of hand graing while variance^2 is a greater predictor of wrist rotation by significant R^2 comparisons*

We extracted the firing rate in Hz from channels 1 and 6 which we calculated in each channel by counting the number of spikes over a 24,000 element moving window and multiplying by 1.25. The second neural feature was the variance-squared, which we obtained from each channel by calculating the variance over a 1,000 element moving window, averaging over a 20,000 element moving window, normalizing data from each channel, and then squaring each value. For both features channel 1 data most closely aligned with hand grasping intent and channel 6 data most closely aligned with wrist grasping intent. (Fig. 4a).

An ANN was then trained with each neural feature, and ANN output predictions on test data were assessed for accuracy by calculating the coefficients of determination (R^2) among ANN predictions and the intended kinematics. We calculated R^2 values for each neural feature's relationship to each type of motor intent.

Firing frequency yielded significantly ($p < 0.001$) more accurate predictions of hand grasping ($R^2 = 0.7123 \pm 0.004$ to $R^2 = 0.6215 \pm 0.0037$) while variance^2 yielded significantly ($p < 0.001$) more accurate predictions of wrist rotation ($R^2 = 0.3000 \pm 0.0173$ to $R^2 = 0.07563 \pm 0.0045$) (Fig. 5).

C. *ANN predictions were most accurate for hand grasping and variance^2 yields continuous predictions*

Subjectively, both features appear to predict hand rotations with fair accuracy but have poor predictive value for wrist rotations (Fig 4b.). Despite intended kinematics consisting of continuous values, due to the firing rate equation making all firing rate values integer multiples of 1.25, the firing rate feature predictions have a "step-wise" and discrete appearance, while variance^2 yields continuous predictions.

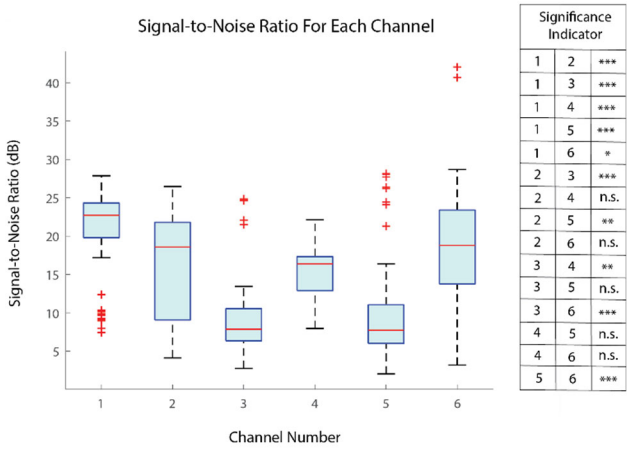

Significance Indicator		
1	2	***
1	3	***
1	4	***
1	5	***
1	6	*
2	3	***
2	4	n.s.
2	5	**
2	6	n.s.
3	4	**
3	5	n.s.
3	6	***
4	5	n.s.
4	6	n.s.
5	6	***

Figure 3. Six channels of neural data obtained from a USEA implanted in the residual median arm nerve of an amputee have average SNRs ranging from 8.9742 dB to 21.0016 dB. The channel SNR averages and standard of error ranges are as follows – Channel 1: 22.7313 (19.7900, 24.3257), Channel 2: 18.5668 (9.0805, 21.7921), Channel 3: 7.8637 (6.3570, 10.5471), Channel 4: 16.3945 (12.8879, 17.3291), Channel 5: 7.7265 (6.0127, 11.0485), Channel 6: 18.7726 (13.7616, 23.4047). Statistical significance as determined by p-value classifications are displayed in the significance indicator above (n.s.: $p > 0.05$, *: $0.05 > p > 0.01$, **: $0.01 > p > 0.001$, ***: $p < 0.001$) and were obtained via a non-parametric ANOVA followed by a multiple comparison test

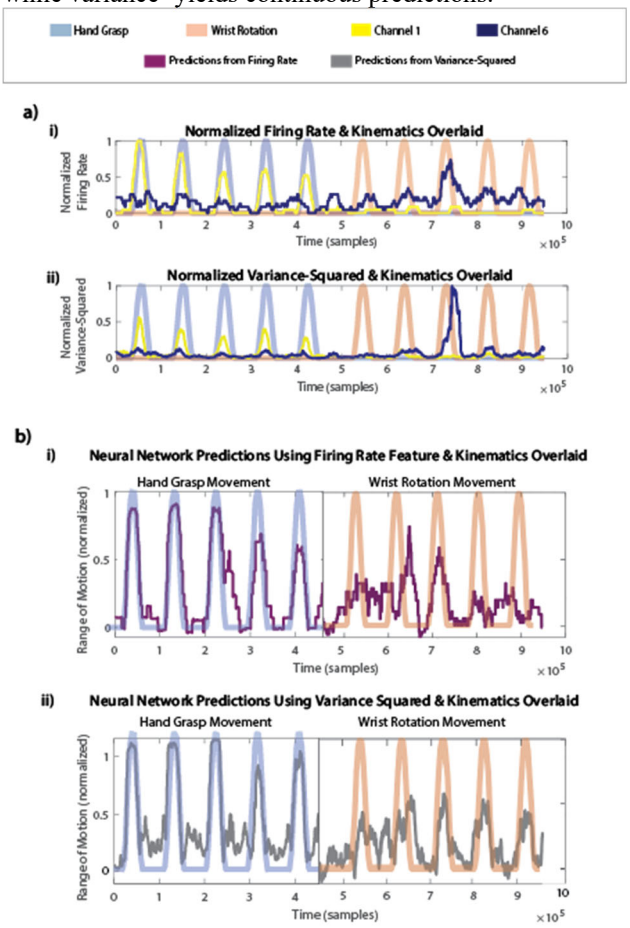

Figure 4. *Voltages from* USEA channels 1 and 6 *and ANN* predictions from both firing rate and variance^2 align somewhat with intended kinematics. Light blue and salmon lines represent hand grasp and wrist rotation *intent*, respectively. Yellow and navy lines represent filtered neural data from USEA channels 1 and 6, respectively. Dark purple and grey lines represent ANN predictions from firing rate and variance^2 features, respectively. Plot a.i. shows the overlay of the firing rates derived from channels 1 and 6 on intended *kinematics*. Plot a.ii. shows the overlay of variance^2 derived from channels *1 and 6* on *intended kinematics*. Plot b.i. shows the overlay of ANN predictions derived from firing rates of channels 1 and 6 on intended *kinematics*. Plot b.ii. shows the overlay of ANN predictions derived from the variance^2 of channels 1 and 6 *on intended kinematics.*

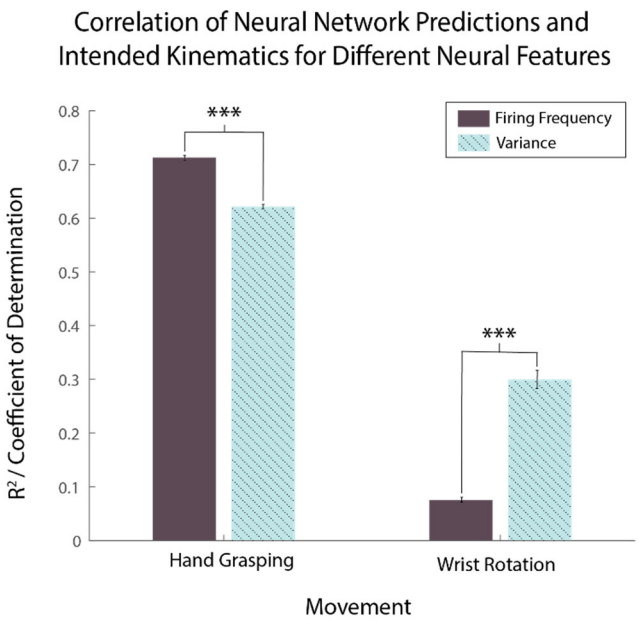

Figure 5. Firing frequency as a neural feature is a superior predictor of hand grasping, while variance of neural data is a superior predictor of wrist rotation, when used as input to our ANN. R^2 values (coefficient of determination) of the relationship between intended kinematics and ANN predictions using firing frequency are represented by the solid dark purple bars, while. R^2 values of the relationship between intended kinematics and ANN predictions using variance of neural data are represented by the striped light blue bars. The average R^2 of the intended kinematics of hand grasping to ANN predictions from firing frequency and variance were 0.7123±0.004 and 0.6215±0. 0037, respectively, while the average R^2 of the intended kinematics of wrist rotation to ANN predictions from firing frequency and variance were 0.07563±0.0045 and 0.3000±0.0173, respectively. We determined statistical significance among R^2 values of the neural features via unpaired t-tests, and obtained p-values < 0.001 for both hand grasping and wrist rotation movements.

IV. Discussion

Our objective was to extract features from a peripheral nerve USEA recording to decode motor intent via an ANN. We found that the two channels with the greatest SNRs could be used as predictors of hand kinematics,. Firing rate neural features yielded more accurate predictions of hand grasping than variance^2, and variance^2 neural features yielded more accurate ANN predictions of wrist rotation than firing rate. Lastly, we observed that ANN predictions were more accurate for hand grasping than wrist rotation and that variance^2 input yields continuous predictions

Prior work with USEAs in peripheral nerves has typically focused on somatosensation, while acknowledging the challenge of decoding motor signals with adjacent sensory signals [6]. The rare motor research has focused on discrete decoders. Here we demonstrate two methods of neural feature extraction (one continuous) for training an ANN to make intended kinematic predictions from peripherally implanted USEA recordings.

The work presented here builds off participant data collected by (Page et al.) [8], spike detection techniques by George et al. [5], and analysis of the limitations of intrafascicular recording techniques by Warren et al [6]. Also novel from this work is the continuous decoding of motor signals from a peripheral nerve via obtaining variance^2 as a neural feature.

Future work should investigate why hand grasping was predicted more accurately than wrist rotation. Furthermore, future work should investigate other neural features that may better decode wrist rotation. Lastly, future work should examine the wide range of SNRs in channels from the same USEA implant.

This study provides the field of neuroprostheses with a two strategies of neural feature extraction from a peripherally implanted USEA to predict motor intent. These results may help electrophysiologists optimize adjust recording techniques for decoding motor intent. Most importantly, this work provides a foundation for improving USEA motor decoding from peripheral nerves, which may ultimately lay the framework for more accessible and advanced neuroprostheses.

Author Contributions

DL and KK digitally filtered USEA data and implemented spike detection together. DL independently developed ideas for and wrote the code to collect and analyze signal-to-noise ratios, obtain neural features, and assess the predictive performance of the neural features. DL created and edited all figures. DL, KK, and LS wrote individual manuscripts.

References

[1] M. P. Fahrenkopf, N. S. Adams, J. P. Kelpin, and V. H. Do, "Hand Amputations.," *Eplasty*, vol. 18, p. ic21, 2018.

[2] E. Noce et al., "EMG and ENG-envelope pattern recognition for prosthetic hand control," Journal of Neuroscience Methods, vol. 311, pp. 38–46, Jan. 2019, doi: 10.1016/j.jneumeth.2018.10.004.

[3] A. L. Ciancio et al., "Control of prosthetic hands via the peripheral nervous system," Frontiers in neuroscience, vol. 10, p. 116, 2016.

[4] C. M. Oddo et al., "Intraneural stimulation elicits discrimination of textural features by artificial fingertip in intact and amputee humans," elife, vol. 5, p. e09148, 2016.

[5] J. A. George et al., "Long-term performance of Utah slanted electrode arrays and intramuscular electromyographic leads implanted chronically in human arm nerves and muscles," J Neural Eng, vol. 17, no. 5, p. 056042, Oct. 2020, doi: 10.1088/1741-2552/abc025.

[6] D. J. Warren et al., "Recording and decoding for neural prostheses," Proceedings of the IEEE, vol. 104, no. 2, pp. 374–391, Feb. 2016, doi: 10.1109/JPROC.2015.2507180.

[7] "Brain Initiative." https://braininitiative.nih.gov/ (accessed Oct. 23, 2022).

[8] [6] D. M. Page et al., "Motor Control and Sensory Feedback Enhance Prosthesis Embodiment and Reduce Phantom Pain After Long-Term Hand Amputation," Frontiers in Human Neuroscience, vol. 12, 2018, Accessed: Oct. 23, 2022. [Online]. Available: https://www.frontiersin.org/articles/10.3389/fnhum.2018.00352

[9] S. Wendelken *et al.*, "Restoration of motor control and proprioceptive and cutaneous sensation in humans with prior upper-limb amputation via multiple Utah Slanted Electrode Arrays (USEAs) implanted in residual peripheral arm nerves," *Journal of NeuroEngineering and Rehabilitation*, vol. 14, no. 1, p. 121, Nov. 2017, doi: 10.1186/s12984-017-0320-4.

[10] X. Xie et al., "Bi-layer encapsulation of utah array based nerual interfaces by atomic layer deposited Al2O3 and parylene C," 2013 Transducers & Eurosensors XXVII: The 17th International Conference on Solid-State Sensors, Actuators and Microsystems (TRANSDUCERS & EUROSENSORS XXVII), pp. 1267–1270, 2013.

[11] D. Lopez, I. Kahnlein, "Improved Virtual Hand Grasping via Discrete, High-Gain Control Algorithm", ECE 6654